Random sequential adsorption of polyatomic species

2007 J. Phys. A: Math. Theor. 40 11765

(http://iopscience.iop.org/1751-8121/40/39/005)

IOP PUBLISHING JOURNAL OF PHYSICS A: MATHEMATICAL AND THEORETICAL

J. Phys. A: Math. Theor. **40** (2007) 11765–11776 doi:10.1088/1751-8113/40/39/005

Random sequential adsorption of polyatomic species

V Cornette, D Linares, A J Ramirez-Pastor and F Nieto

Departamento de Física, Universidad Nacional de San Luis, CONICET, Chacabuco 917, D5700BWS San Luis, Argentina

E-mail: cornette@unsl.edu.ar, dlinares@unsl.edu.ar, antorami@unsl.edu.ar and fnieto@unsl.edu.ar

Received 20 March 2007, in final form 8 August 2007
Published 11 September 2007
Online at stacks.iop.org/JPhysA/40/11765

Abstract

Random sequential adsorption of k-mers (particles occupying k adsorption sites on the substrate) of different sizes and shapes deposited on two-dimensional regular lattices is studied. For discrete models at the late stage the surface coverage evolves according to $\theta(t) = \theta(\infty) - A\exp\left[-\frac{t}{\sigma}\right]$, where $\theta(\infty)$ is the jamming coverage while A and σ are fitting parameters. In the present paper, the dependence of the terminal relaxation time σ (which determine how fast the lattice is filled up to the jamming coverage) on the parameters of the problem is established through a theoretical approach. In addition, a strategy for determining σ by means of a computational algorithm is presented.

PACS numbers: 02.50.Ey, 68.43.Mn, 68.43.−h, 02.70.Uu

1. Introduction

Random sequential adsorption (RSA) is the irreversible process by which particles of different shapes and sizes are deposited on a discrete or continuous surface. The assumptions of the RSA models are easily stated: objects are placed randomly one after another in a d-dimensional volume [1]. In case that the last placed object overlaps with any of those already present, it is immediately removed; otherwise its position is permanently fixed. These models have been applied to a significative number of systems where the deposition of objects is irreversible over time scales of physical interest. Among others, a variety of physical [2], chemical [3], biological [4–6] and ecological [7] processes have been modeled by using an RSA scheme.

Reversible adsorption has been explored using equilibrium statistical mechanics, and a variety of information on the correlation among the adsorbed species is known [8]. The irreversible RSA problem represents a nonequilibrium situation which is fundamentally different. The earliest exact results come from Flory's statistical analysis of saturation coverage for random filling in one-dimensional lattices [9]. In one dimension, other seminal contributions describing RSA develop exact results [10, 11]. However, for the general problem

on higher dimensional lattices one only has approximate solutions and numerical approaches emerge as an important tool in order to obtain the behavior of the model. Thus, although the problem of RSA is an old one [9–14], it has recently been attracting renewed interest [15–24].

The kinetics of the process is characterized by the time evolution of the coverage (or the density of the system), $\theta(t)$, i.e. the fraction of the substrate covered by the deposited objects. This dependence has been the object of analysis during the last decades. In previous theoretical studies of RSA, which include Monte Carlo approaches [25–29], series expansion [27, 30, 31], rate equations [26, 28, 32], etc, both continuous and discrete models were analyzed. In such studies it was established that the late stage deposition kinetics follows either a power law (for continuous models) or an exponential function (for discrete models) approach to the jamming limit. Thus, for discrete models, one writes for long times

$$\theta(t) = \theta(\infty) - A \exp\left[-\frac{t}{\sigma}\right], \tag{1}$$

where $\theta(\infty)$ is the jamming coverage, while A and σ are fitting parameters. In continuous models the description of the process is quite different. For the deposition of disks on continuum, numerical results as well as theoretical analyses suggest that the coverage follows $\theta(\infty) - \theta(t) \sim t^{-p}$, where $p = 1/d$ and d is the dimensionality of the host space. This result was first conjectured by Feder (known as Feder's law) [5] and later proved by Pomeau [33] and Swendsen [34]. However, it is important to emphasize that for nonspherical particles, Feder's law is not obeyed with $p = 1/d$, and an effective value of p must be defined which depends on the shape of the deposited object [28, 35].

Several papers have discussed the dependence of the parameter σ (which determine how fast the lattice is filled up to the jamming coverage) on the main features of the system under consideration: shape and size of the adsorbing object, symmetry of the substrate, etc. We shall cite in the following some of the results presented in the last years. In [36], it is stated that σ depends on the shape and size of the adsorbing object in agreement with the analytical results of Gonzales *et al* [11]. The deposition of lines or needles of different lengths is discussed in [17, 30]. It is concluded by numerical simulations that σ depends on the order of symmetry of the shape. The rate σ does not depend on the length of the needle. RSA of objects of various shapes on a planar triangular lattice studied by means of Monte Carlo simulations is reported in [18]. It is claimed that σ depends mostly on the order of symmetry of the shape. Deposition of mixtures of objects with different shapes [17] as well as the influence of impurities on the lattice have also been considered [36].

The main purpose of the present paper is to determine the dependence of the rate σ with the parameters of the problem and, in turn, to develop a numerical strategy to calculate it from Monte Carlo simulations. In order to corroborate the theoretical predictions, we shall present numerical results of RSA on different two-dimensional regular lattices.

The paper is organized as follows. In section 2 we describe a theoretical approach in order to determine the dependence of the exponent σ on the order of symmetry of the depositing object. The model and the numerical technique used in the Monte Carlo simulations are described in section 3. Results are presented and discussed in section 4. Finally, the concluding remarks are given in section 5.

2. Theoretical approach

The dependence of surface coverage on time $\theta(t)$ can distinguish three different regimes. At short times, the deposited particles are, on average, enough far apart between them. Then, each attempt to deposit a new particle is successful. Thus, the deposition events are largely

uncorrelated and $\theta(t) \propto t$. In this regime, mean field like low density approximation schemes are useful [5, 11, 37]. At very long times, the surface coverage reaches its saturation value (the jamming coverage) and it remains constant. In this situation only gaps smaller than the particle size are left in the monolayer. The resulting jammed state is less dense than the fully ordered close-packed coverage.

Let us consider now the state of the system at large enough time (t^*) in such a way that few k-mers left to be deposited in order to reach the jammed state. At this moment, the empty sites can be sorted in two groups: (a) those in which a single k-mer can be deposited and (b) those which are simple *dead sites* (where it is not possible to deposit any k-mer). The evolution of the empty sites, ΔN, can be described by

$$\Delta N = -P_{\mathrm{ad}}\, k \Delta\eta, \tag{2}$$

where P_{ad} is the adsorption probability and $\Delta\eta$ is the number of deposition attempts. Defining the Monte Carlo unit of time to be N_t ($N \times N$) attempts for deposition, we can rewrite equation (2) as

$$\Delta N = -P_{\mathrm{ad}}\, k N_t \Delta t, \tag{3}$$

where $\Delta t = \Delta\eta/N_t$. The adsorption probability can be given by

$$P_{\mathrm{ad}}(t) = \frac{\sum_i g_i(t)}{\sum_i g_i^{\max}}, \tag{4}$$

where $g_i^{\max}$ and $g_i(t)$ can be understood as follows. Once a k-mer's end is deposited on a site i, there exists $g_i^{\max}$ ways of adsorbing this object at zero density, with $g_i^{\max}$ being a measure of the lattice/k-mer geometry (for instance, straight k-mers adsorbed on a square lattice would correspond to $g_i^{\max} = 4$). At a given time t, some states out of $g_i^{\max}$ are prevented from occupation upon adsorption of another object. Thus, the number of configurations (among the set of total ways, i.e. $g_i^{\max}$) which lead to adsorbed states is denoted as $g_i(t)$ $\left(g_i(t) \leqslant g_i^{\max}\right)$. If the lattice is homogeneous, $\sum_i g_i^{\max}$= constant = $N_t\langle g^{\max}\rangle$=$N_t g^{\max}$.

At the late stage of the filling process, we can distinguish clusters of empty sites where k-mers can be deposited. We denote with c_j such clusters and then

$$\sum_i g_i(t) = \sum_j \left[\sum_{i\in c_j} g_i(t)\right], \tag{5}$$

where the '*degrees of freedom*' of the cluster, $G_j(t)$, are defined as

$$G_j(t) = \sum_{i\in c_j} g_i(t). \tag{6}$$

Then, by using the above equations, we rewrite equation (4) as

$$P_{\mathrm{ad}}(t) = \frac{\sum_j G_j(t)}{N_t\langle g^{\max}\rangle} = \frac{N_{\mathrm{clus}}(t)\langle G(t)\rangle}{N_t\langle g^{\max}\rangle}, \tag{7}$$

with $N_{\mathrm{clus}}(t)$ being the number of clusters of empty sites at time t where a k-mer can be deposited. Now, equation (3) becomes

$$\Delta N = -\frac{N_{\mathrm{clus}}(t)\langle G(t)\rangle}{\langle g^{\max}\rangle} k \Delta t. \tag{8}$$

For large enough times, we assume that

$$N(t) - N(\infty) = N_{\mathrm{clus}} k. \tag{9}$$

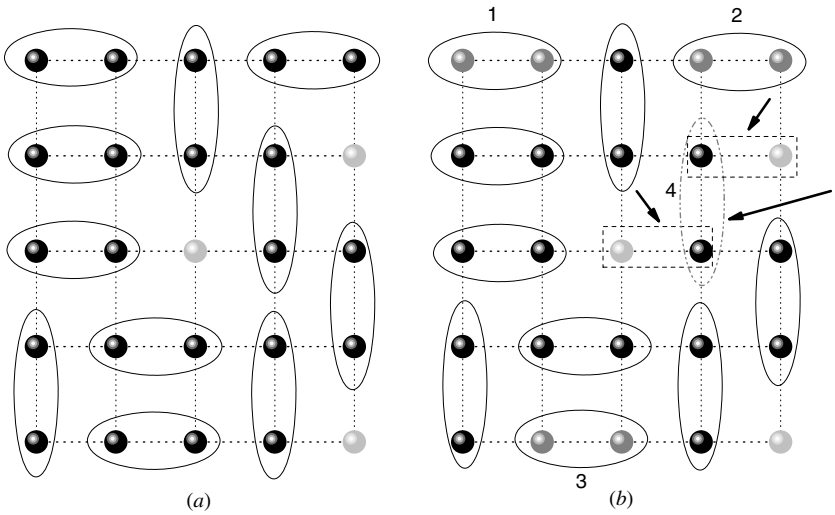

Figure 1. (*a*) An example of the jammed state for deposition of dimers on a square lattice. (*b*) Illustration of the second step of the proposed algorithm for calculating the effective activity of the lattice according to what is described in the text (section 3).

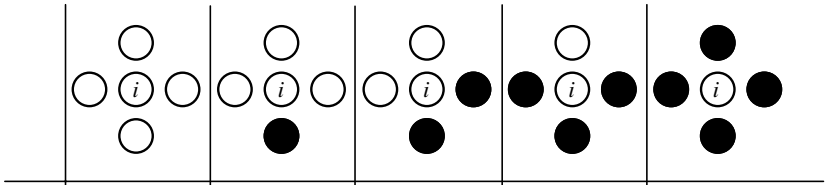

standard model	$P_i(t)$ =1.0 $g_i(t)$ = 4.0	$P_i(t)$ = 3/4 $g_i(t)$ = 3.0	$P_i(t)$ = 1/2 $g_i(t)$ = 2.0	$P_i(t)$ =1/4 $g_i(t)$ = 1.0	$P_i(t)$ =0.0 $g_i(t)$ = 0.0
end-on model	$P_i(t)$ =1.0 $g_i(t)$ = 4.0	$P_i(t)$ =1.0 $g_i(t)$ = 4.0	$P_i(t)$ =1.0 $g_i(t)$ = 4.0	$P_i(t)$ =1.0 $g_i(t)$ = 4.0	$P_i(t)$ =0.0 $g_i(t)$ = 0.0

Figure 2. An attempt for deposition of a dimer on the site i in five different configurations. $P_i(t)$ and $g_i(t)$ are calculated for each situation and for the standard and the end-on RSA scheme, $g_i^{\max} = 4$.

Thus, by considering the above equations and $\mathrm{d}N(t) = \mathrm{d}[N(t) - N(\infty)]$, we have

$$\Delta \underbrace{[N(t) - N(\infty)]}_{z} = -\underbrace{[N(t) - N(\infty)]}_{z} \underbrace{\frac{\langle G(t)\rangle}{\langle g^{\max}\rangle}}_{F(=\text{constant})} \Delta t. \tag{10}$$

In short, the last equation can be written as

$$\Delta z = -Fz\Delta t, \tag{11}$$

or

$$\frac{\mathrm{d}z}{\mathrm{d}t} = -F \cdot z. \tag{12}$$

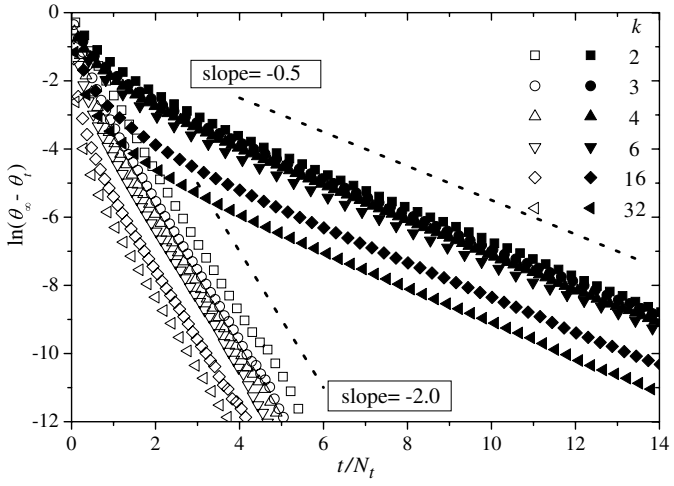

Figure 3. $\ln[\theta_\infty - \theta(t)]$ as a function of t/N_t for deposition of linear k-mers on a square lattice. The parameter θ_∞ is fitted in such a way that the resulting curve for long times is linear. The slope of the resulting curve determines the parameter σ. $\sigma = 2.0$ ($F = 0.5$) for the standard RSA model while $\sigma = 0.5$ for the end-on model ($F = 2.0$), as indicated.

By integrating equation (12) for times larger than a given large enough value, t^*:

$$\theta(\infty) - \theta(t) = [\theta(\infty) - \theta(t^*)]\, \mathrm{e}^{-F(t-t^*)}, \tag{13}$$

or

$$\theta(\infty) - \theta(t) = A\, \mathrm{e}^{-Ft}, \tag{14}$$

where $A = [\theta(\infty) - \theta(t^*)]\, \mathrm{e}^{-Ft^*}$ is the integration constant.

Thus, one finally obtains

$$\theta(t) = \theta(\infty) - A\, \mathrm{e}^{-Ft}. \tag{15}$$

This equation describes the time evolution of the surface coverage in the close vicinity of the jamming coverage. Note that (a) equations (1) and (15) have the same form, and (b) it is possible to explicitly obtain the dependence of the exponent F as

$$F = \frac{1}{\sigma} = \frac{\langle G(t) \rangle}{\langle g^{\max} \rangle}. \tag{16}$$

Thus, if the depositing object and the geometry of the substrate are known, then equation (16) predicts the value of the exponent σ.

3. Simulation details

In this section we propose an algorithm for calculating the exponent F defined by equation (16) and henceforth called 'effective activity'. In order to measure this quantity as a function of time (at enough large times) we have developed the following strategy:

(1) k-mers are deposited until the jamming coverage is reached. In several cases, the obtained results can be compared with theoretical or numerical values reported in the literature. The deposited k-mers are identified by consecutive numbers.

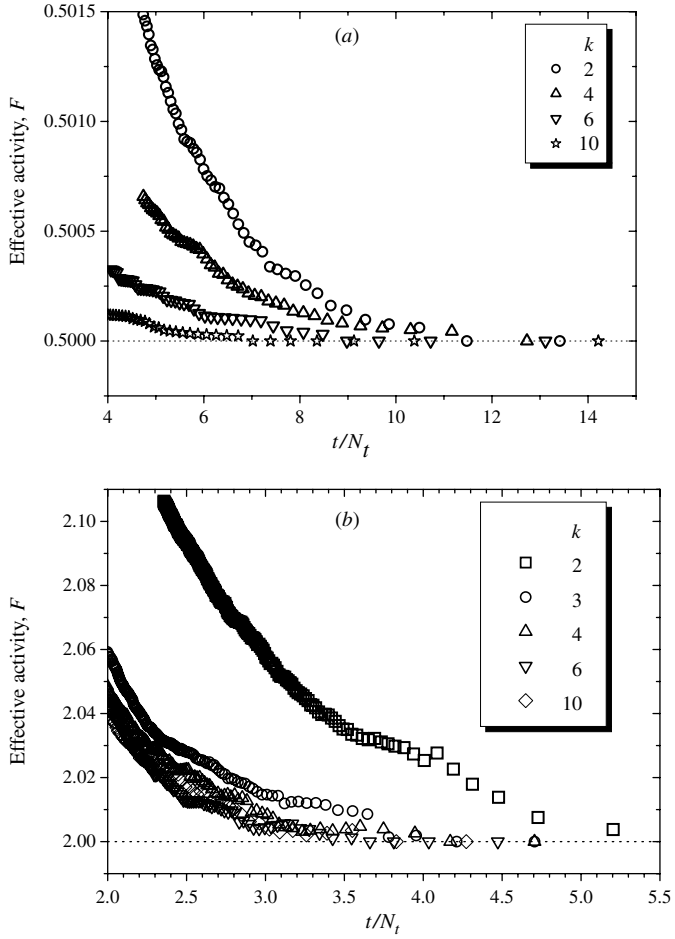

Figure 4. Effective activity for deposition of linear k-mers on a square lattice as a function of time as indicated. One Monte Carlo time step was defined by the total number of attempts to select a site divided by the total number of lattice sites. Results for (*a*) the standard scheme and (*b*) the end-on model.

(2) Once the jamming state is reached, the last deposited k-mers are removed with the following criterion: a k-mer will be removed only if a unique k-uple of the remaining empty sites can be used for depositing a new k-mer.

Figure 1 illustrates this procedure. The last four adsorbed dimers are labeled. The last deposited dimer (labeled with number 1) is removed. Its neighbors are all occupied, and then only a dimer in the horizontal direction can be deposited in the vacant area. Next, we consider the situation of the dimer labeled with the number 2. It possesses three empty nearest neighbor (remember we are using periodic boundary conditions). If that dimer is removed, a unique dimer can be deposited with the condition that one of its monomers can be deposited on the recently vacant sites. Dimer 2 is removed. k-mer 3 has only one empty nearest neighbor (after removing dimer 1) and it will be removed. Dimer 4 possesses three empty nearest neighbor sites (after removing dimer 2) but their distribution makes possible the deposition of two dimers where only a dimer was deposited before. The process is stopped at this point.

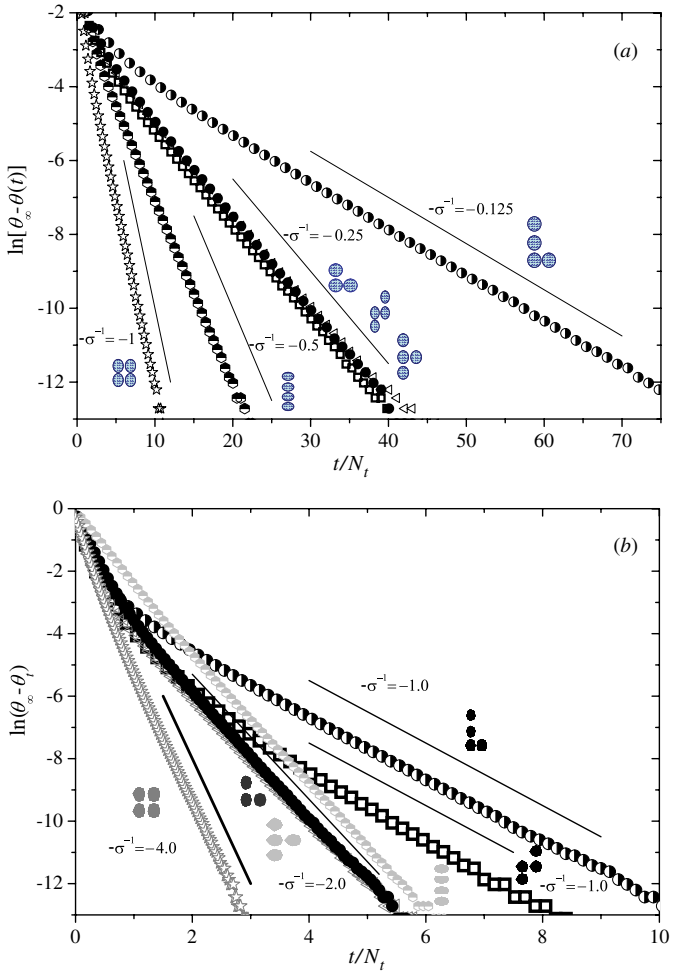

Figure 5. Idem figure 3 for bent trimers and five different shapes of tetramers, as indicated. Close to each shape considered, the calculated value of σ is also included. (*a*) Standard and (*b*) end-on model.

(3) Each times that a k-mer is removed (which was previously deposited at time t), the effective activity of the lattice at time t is calculated, updated and averaged over n realization of the experiment.

We have chosen a number of different realizations of the experiment in such a way that the effective activity fluctuates lower than 0.5% around its average value. We have consider $n = 5 \times 10^3$ samples for each studied case. The evaluation of the effective activity by the above procedure and the use of equation (16) allow us to determine the kinetic exponent σ.

4. Results and discussion

We start our analysis by considering the deposition of linear k-mers on a square lattice. In order to compare our results with the previous ones in the literature, we perform a standard simulation of RSA. For such purpose, we have used two simulation schemes.

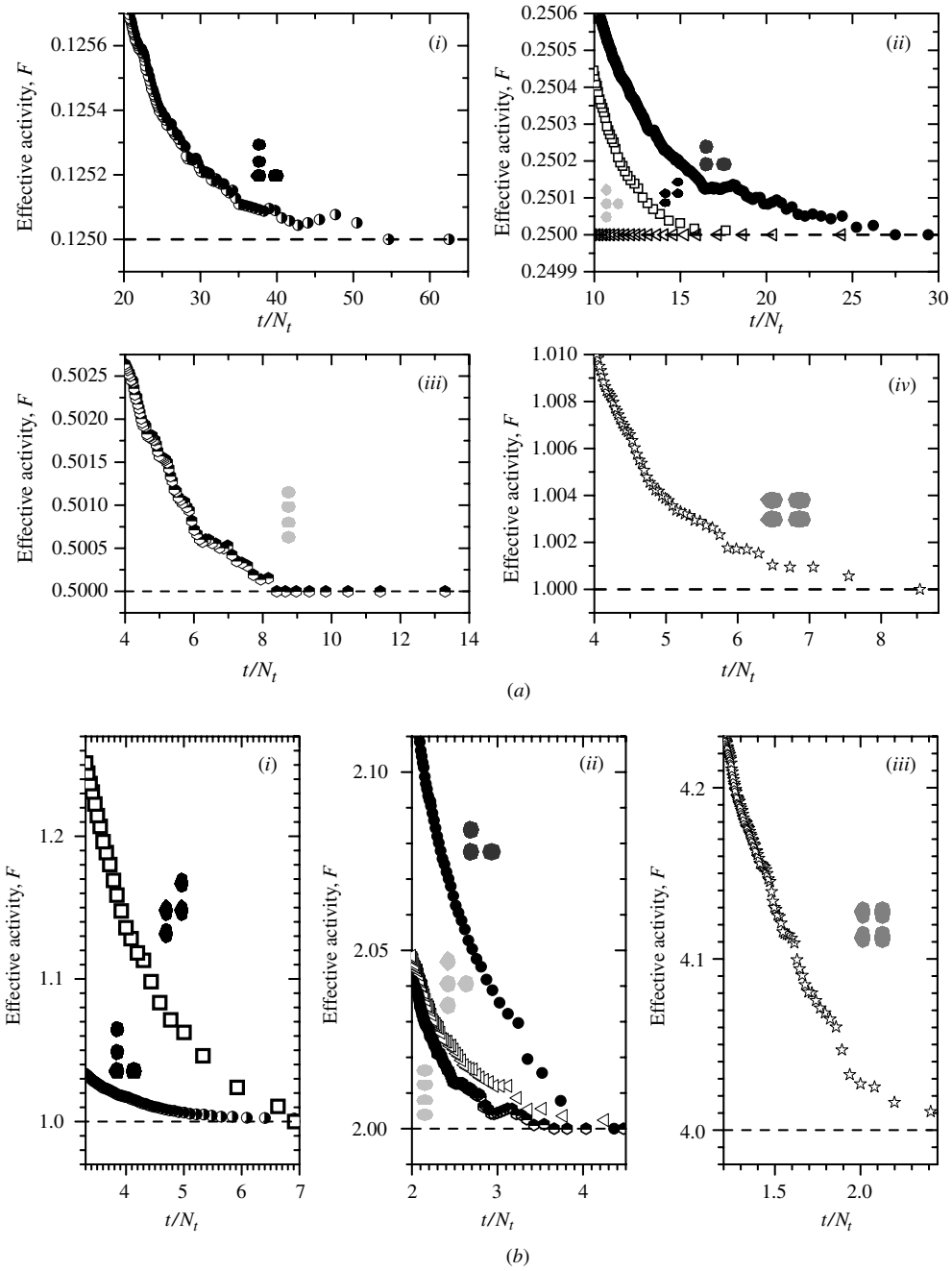

Figure 6. Effective activity as a function of time for each one of the k-mers discussed in figure 5, as indicated. The effective area converges for enough large times towards the same values of those reported in figures 5(*a*) and (*b*). (*a*) Standard and (*b*) end-on models.

First, we randomly select a site. If the chosen site is occupied by an already deposited object, the attempt fails and time is increased by one unit. If the chosen site is empty, then we randomly select a direction from the z possible orientations (four in the case of the

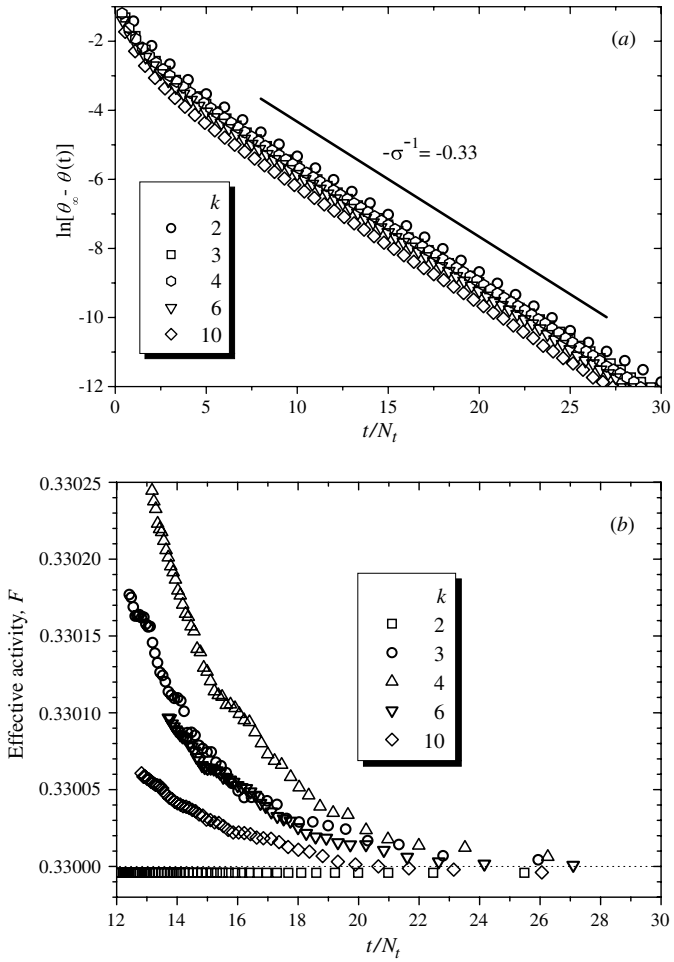

Figure 7. Idem to (*a*) figure 3(*a*) and (*b*) figure 4(*a*); for deposition of linear *k*-mers on a triangular lattice, as indicated.

square lattice) regardless of the occupation of the neighbor sites. Thus, it is possible to reject deposition of the selected line segment even if there are empty consecutive neighbor sites for the chosen line segment. If any neighbor site is occupied by a previously deposited object, in a chosen direction then the attempt fails, the time is increased by one unit and we try a new site. This scheme is usually called *conventional* or *standard* model of RSA. The second strategy to perform an RSA is named *end-on* model. Here, we check the possible directions (unblocked directions) of the chosen site and select a possible direction. We deposit the chosen line segment in the selected direction. When there is at least an unblocked direction, the deposition is always carried out in the *end-on* model. The theoretical model introduced in section 2 can be adapted to both schemes. In order to clarify this point, it is convenient to write $g_i(t)$ as

$$g_i(t) = P_i(t) g_i^{\max}, \tag{17}$$

where $P_i(t)$ is the probability of occurrence of an adsorbed state (with the *k*-mer's end at the site *i*) in a time unit (between t and $t + 1$). Thus, it is clear that $P_i(t)$ also depends on the

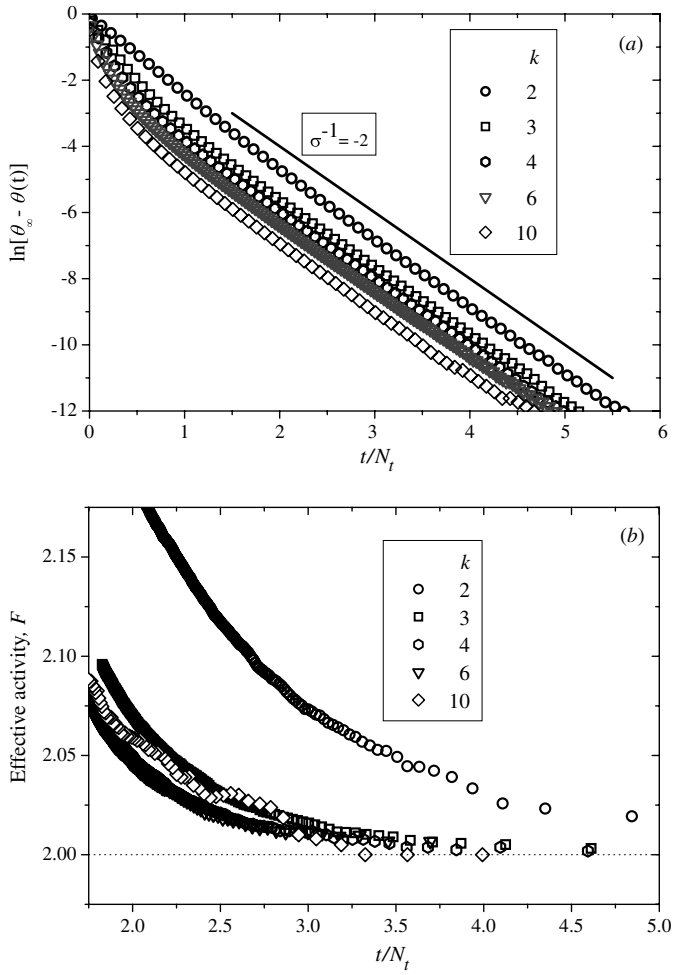

Figure 8. Idem to (*a*) figure 3(*b*) and (*b*) figure 4(*b*); for deposition of linear *k*-mers on a triangular lattice, as indicated.

simulation scheme used for deposition. As an example of how the theory can be applied, in figure 2 we consider the deposition of a dimer on the site i in different configurations. $P_i(t)$ and $g_i(t)$ are calculated for each situation and scheme. Since the above analysis, we can conclude that the exponent σ depends on both the lattice/k-mer geometry or *degree of freedom* that the depositing object possesses and the simulation scheme used for deposition.

Based on Monte Carlo simulations it is very well known in the literature [20, 38] that (a) σ is independent of the size of the depositing species (b) $\sigma = 2$ ($F = 0.5$) for the standard model and (c) $\sigma = 0.5$ ($F = 2.0$) for the end-on model. The standard procedure to determine σ consists in plotting $\ln[\theta_\infty - \theta(t)]$ as a function of t/N_t, by fitting the parameter θ_∞ in such a way that the resulting curve for long times is linear (see figure 3). This procedure is very sensitive and allows a very accurate determination of θ_∞. The slope of the resulting curve determines the parameter σ which has been found to be constant for all the cases studied here regardless the k-mer sizes. $\sigma = 2.0$ for the standard RSA model means that at large times the

deposition of k-mers occurs in only one direction ($F = 0.5$). For the *end-on* model $\sigma = 0.5$ ($F = 2.0$).

It is of interest to compare the standard determination of the exponent σ (figure 3) with our predictions (based on the theoretical framework presented in section 2 and the numerical procedure discussed in section 3). For this purpose, in figure 4 the effective activity is presented as a function of time for (a) the standard model and (b) the end-on scheme. For enough large times, F converges to value 0.5 (2.0) for the standard (end-on) model, regardless the size of the k-mer.

The next case to be analyzed is the RSA of k-mers of different shapes and sizes. In figure 5, we present the curves $\ln[\theta_\infty - \theta(t)]$ as a function of t/N_t for bent trimers and five different shapes of tetramers for (a) the standard and (b) the end-on models. Close to each shape considered, the calculated value of σ is included. The same problem can be treated in terms of our model. Figure 6 shows the effective activity for each one of the k-mers discussed in figure 5 as a function of time and for the two mechanisms of deposition considered: (a) standard and (b) end-on model. For enough large times, the effective area converges to the same values of those reported in figure 5.

Finally, we consider the deposition of linear k-mers on a triangular lattice where $g_i^{\max} = 6$. Figures 7(a) and (b) (8(a) and (b)) show the curve of $\ln[\theta_\infty - \theta(t)]$ as a function of t/N_t and the temporal evolution of the effective activity, respectively, for the standard (end-on) scheme. Figures confirm the predicted value of $\sigma = 3$ and $\sigma = 0.5$ for the standard and the end-on scheme, respectively. These values agree with previous reports in the literature [18].

5. Conclusions

In the present paper we have determined the dependence of the terminal relaxation time σ on both the lattice/k-mer geometry or *degree of freedom* that the depositing object possesses and the simulation scheme used for deposition. The theoretical derivation of such dependence allows us to develop a numerical strategy for calculating σ directly from Monte Carlo simulations.

In order to corroborate the theoretical predictions, we have presented numerical results of RSA on different regular lattices in two-dimensional systems. In such tests, the exponent σ can be additionally obtained from the slope of the curve $\ln[\theta_\infty - \theta(t)]$ as a function of t/N_t. This 'traditional' derivation of σ allows us to compare our results obtained via the calculation of the effective activity. This concept is derived from the theoretical approach presented in section 2. The agreement between these two strategies is excellent and allows us to predict the expected value of the exponent σ in all cases considered here.

These findings encourage us for using the proposed scheme to evaluate σ in cases where (a) the calculus of the active area is more simple than the traditional way and/or (b) the interpretation of the results is facilitated. Examples of such problems are the deposition of (i) mixtures of k-mers (especially enantiomeric species), (ii) k-mers on heterogenous substrates (including those which are devoid of translational symmetry: fractals) and (iii) k-mers on diluted lattices [39, 40]. These studies are in progress.

Acknowledgments

This work was supported in part by CONICET (Argentina) under project PIP 6294, Universidad Nacional de San Luis (Argentina) under projects 328501 and 322000 and the National Agency of Scientific and Technological Promotion (Argentina) under project 33328 PICT 2005. The

numerical work was done using the BACO parallel cluster (composed by 60 PCs each with a 3.0 MHz Pentium-4 processors) located at Laboratorio de Ciencias de Superficies y Medios Porosos, Universidad Nacional de San Luis, San Luis, Argentina.

References

[1] Evans J W 1993 *Rev. Mod. Phys.* **65** 1281
[2] Zallen R 1983 *The Physics of Amorphous Solids* (New York: Wiley)
[3] Evans J W, Hoffman D K and Burgess D R 1983 *J. Chem. Phys.* **79** 5011
[4] Epstein I R 1979 *Biopolymers* **18** 765
[5] Feder J 1980 *J. Theor. Biol.* **87** 237
[6] Finegold L and Donnell J T 1979 *Nature* **278** 443
[7] Hasegawa M and Taneumura M 1980 *Recent Developments in Statisical Inference and Data Analysis* ed K Matusita (Amsterdam: North-Holland)
[8] Zgrablich G 1996 *Equilibria and Dynamics of Gas Adsorption on Heterogeneous Solid Surfaces* ed W W Rudzinski and G Zgrablich (Amsterdam: Elsevier)
[9] Flory P J 1939 *J. Am. Chem. Soc.* **61** 1518
[10] Widom B 1966 *J. Chem. Phys.* **44** 3888
[11] Gonzales J J, Hemmer P C and Hoye J S 1974 *Chem. Phys.* **3** 228
[12] Renyi A 1958 *Publ. Math. Inst. Hung. Acad. Sci.* **3** 109
[13] Mackenzie J K 1962 *J. Chem. Phys.* **37** 723
[14] Solomon H 1967 *Proc. 5th Berkeley Symp. Math. Stat. Prob.* vol 3 ed J Neyman (Berkeley, CA: University of California Press) p 119
[15] Baram A and Kutasov D 1989 *J. Phys. A: Math. Gen.* **22** L251
[16] Ziff R and Vigil R D 1990 *J. Phys. A: Math. Gen.* **23** 5103
[17] Budinski-Petković Lj and Kozmidis-Luburić U 1997 *Physica* A **245** 261
[18] Budinski-Petković Lj and Kozmidis-Luburić U 1997 *Phys. Rev.* E **56** 6904
[19] Budinski-Petković Lj and Kozmidis-Luburić U 1999 *Physica* A **262** 388
[20] Lee J W 2000 *Colloids Surf.* A **165** 363
[21] Cortes J and Valencia E 2002 *J. Colloid Interface Sci.* **252** 256
[22] Budinski-Petković Lj and Tošić T 2003 *Physica* A **329** 350
[23] Budinski-Petković Lj, Petković M, Jakšić Z M and Vrhovac S B 2005 *Phys. Rev.* E **72** 046118
[24] Nazzarro M S, Ramirez-Pastor A J, Riccardo J L and Pereyra V 1997 *J. Phys. A: Math. Gen.* **30** 1925
[25] Nakamura M 1987 *Phys. Rev.* A **36** 2384
[26] Schaaf P and Talbot J 1989 *Phys. Rev. Lett.* **62** 175
[27] Vigil R D and Ziff R M 1989 *J. Chem. Phys.* **91** 2599
[28] Talbot J, Tarjus G and Schaaf P 1989 *Phys. Rev.* A **40** 4808
[29] Sherwood J D 1990 *J. Phys. A: Math. Gen.* **23** 2827
[30] Bonnier B, Honterbeyrie M, Leroyer Y, Meyers C and Pommiers E 1994 *Phys. Rev.* E **49** 305
[31] Baram A and Fixman M 1995 *J. Chem. Phys.* **103** 1929
[32] Evans J and Nord R S 1985 *J. Stat. Phys.* **38** 681
[33] Pomeau Y 1980 *J. Phys. A: Math. Gen.* **13** L193
[34] Swendsen R H 1981 *Phys. Rev.* A **24** 504
[35] Wang J-S and Pandey R B 1996 *Phys. Rev. Lett.* **77** 1773
[36] Milošević D and švrakić N M 1993 *J. Phys. A: Math. Gen.* **26** L1061
[37] Dickman R, Wang J-S and Jensen I 1991 *J. Chem. Phys.* **94** 8252
[38] Manna S S and švrakić M N 1991 *J. Phys. A: Math. Gen.* **24** L671
[39] Cornette V, Ramirez-Pastor A J and Nieto F 2006 *Phys. Lett.* A **353** 452
[40] Cornette V, Ramirez-Pastor A J and Nieto F 2006 *J. Chem. Phys.* **125** 2047021